water

MDPI

Article

A Large-Scale 3D Study on Transport of Humic Acid-Coated Goethite Nanoparticles for Aquifer Remediation

Milica Velimirovic [1,2], Carlo Bianco [3], Natalia Ferrantello [3], Tiziana Tosco [3], Alessandro Casasso [3], Rajandrea Sethi [3,*], Doris Schmid [1], Stephan Wagner [1,4], Kumiko Miyajima [5], Norbert Klaas [5], Rainer U. Meckenstock [6], Frank von der Kammer [1] and Thilo Hofmann [1,*]

Supplementary Materials

Table S1. AF4 and ICP-MS operational parameters used for HA-GoeNPs characterization.

AF4	unit	value
Tip to tip channel length	(cm)	27.5
Spacer	(µm)	350
Focus flow rate	(ml/min)	0.60
Injection flow	(ml/min)	0.1
Injection time	(min)	12
Focus time	(min)	2
Elution time	(min)	45
Detector flow rate	(mL/min)	1
Cross flow rate	(mL/min)	0.6
Membrane		Regenerated cellulose (RC), 10 kDa, Nadir
Carrier		0.025% (v/v) FL-70™ , 0.25mM NaCl
Injection volume	(µL)	50 of sample suspension
ICP-MS		
RF power	(W)	1600
Sample depth	(mm)	10
Gas flow rates		
-Carrier	(L/min)	1.06
-Dilution	(L/min)	0.35
-Collision gas He	(mL/min)	4.5
Sample uptake rate	(mL/min)	0.3 (established by split flow)
Nebulizer		MICROMIST (Glass Expansion)
Spray chamber		Scott double-pass
Isotopes monitored		^{56}Fe
Dwell time	(ms)	100

Size calibrations of the AF^4 channel were performed under similar run conditions.

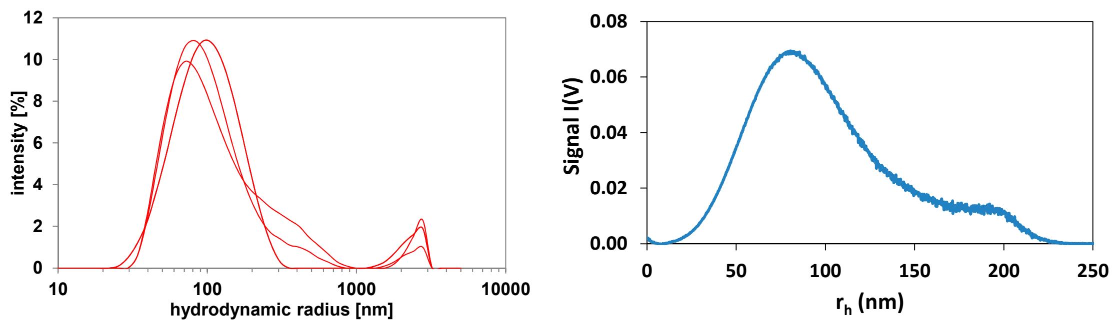

(A) (B)

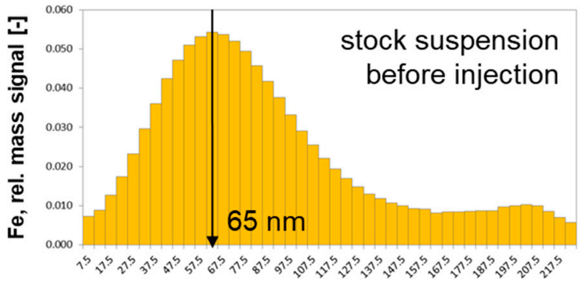

(C)

Figure S1. Characterization of the initial HA-GoeNPs. (**A**) Hydrodynamic radius distributions as estimated with dynamic light scattering (DLS) analysis (triplicate) and (**B**) Hydrodynamic radius as measured by AF4-MALS and (**C**) AF4-ICPMS.

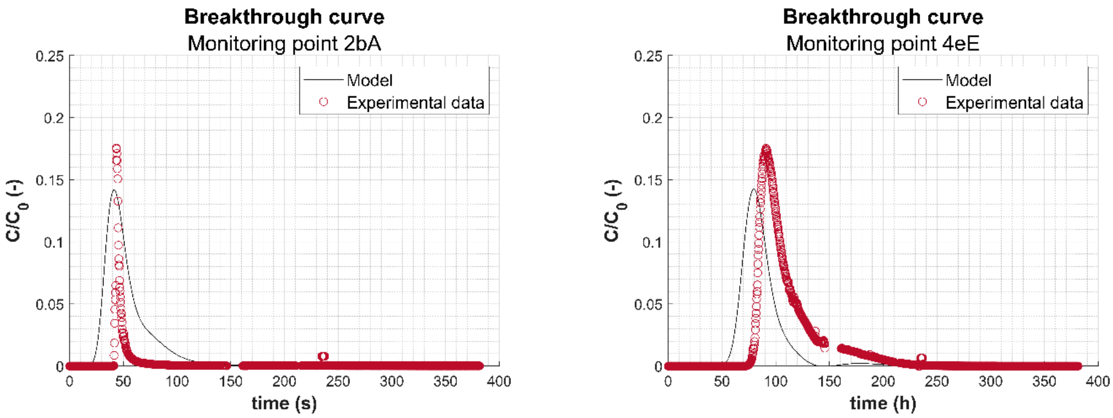

(A) **(B)**

Figure S2. Breakthrough curves of tracer (tracer test) at the monitoring points (**A**) 2bA (x_{2bA} = 1.5 m, y_{2bA} = 5.56 m, z_{2bA} = 3.31 m), (**B**) 4eE (x_{4eE} = 4.5 m, y_{4eE} = 2.12 m, z_{4eE} = 1.84 m).

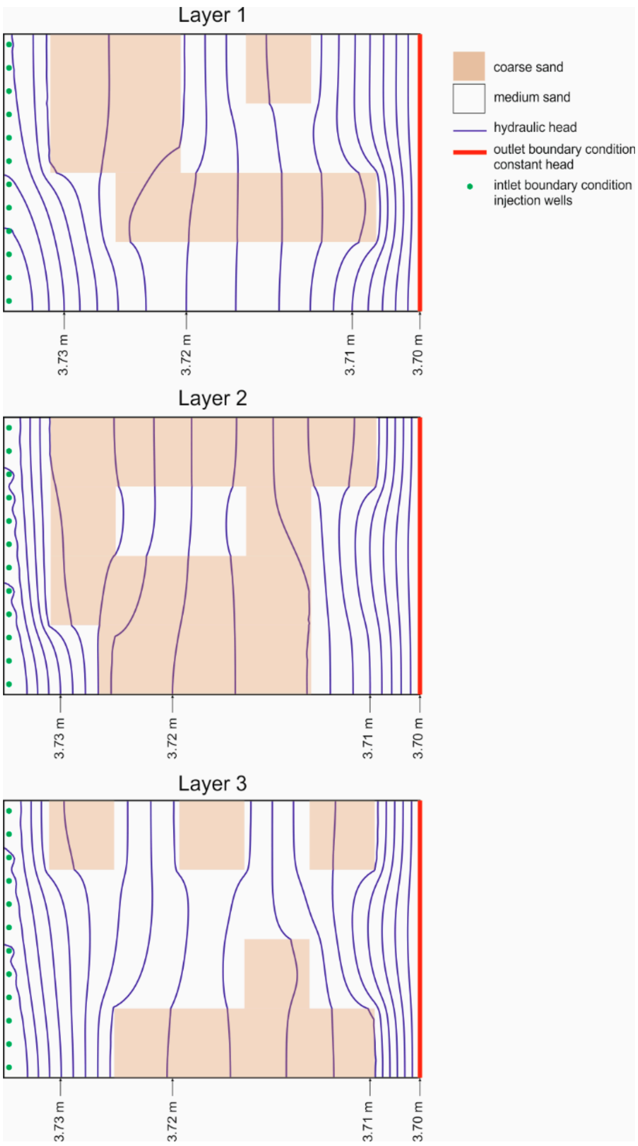

Figure S3. Planar view of the steady state background flow field simulated in Visual Modflow, for the three layers of the large-scale container (numbered from top to bottom, see Figure 1 in the paper). White blocks correspond to medium sand, light brown blocks correspond to coarse sand. Flow direction is from left to right. Boundary conditions: injection wells (each injecting 0.25 m^3/d) are reported in green, downstream constant head boundary is reported in red; no-flow boundaries are applied to all other sides of the model domain, reproducing the stainless steel walls of the container.

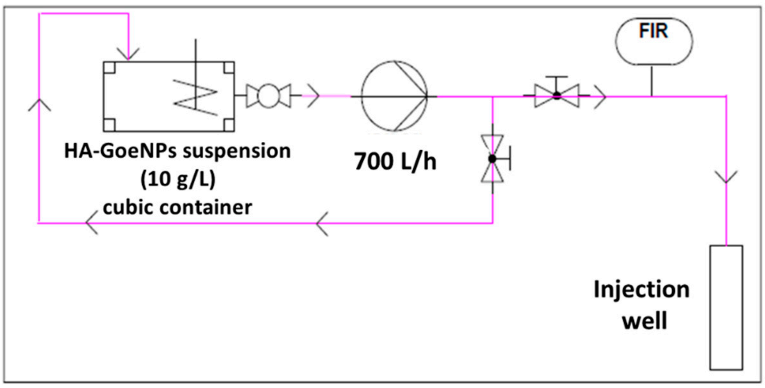

Figure S4. Injection of HA-GoeNPs suspension.

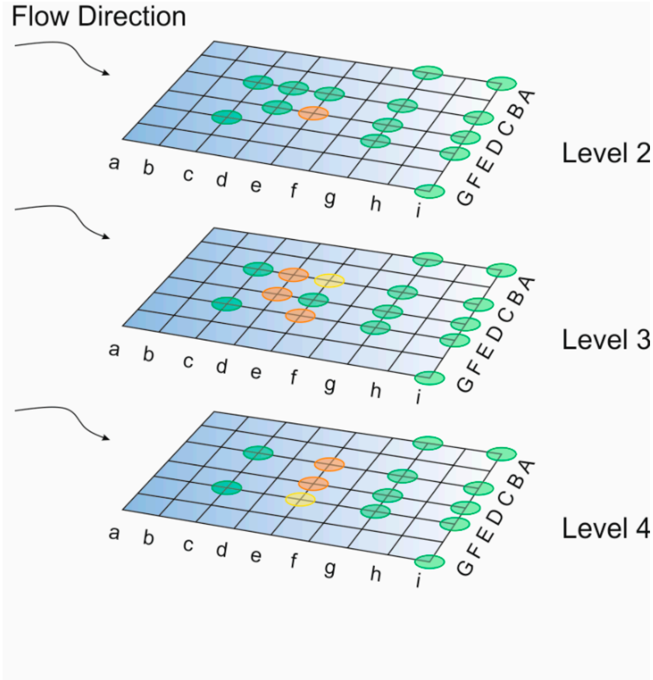

(A)

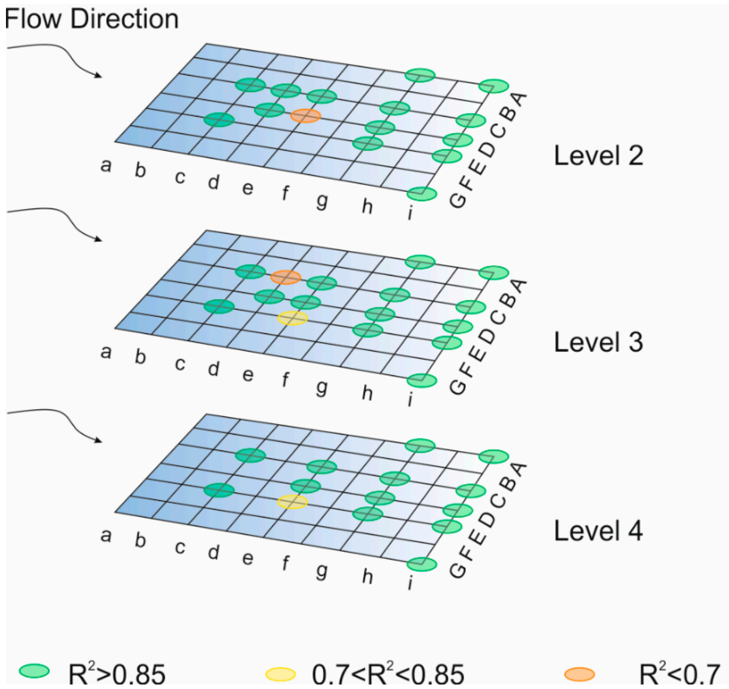

(B)

Figure S5. Spatial distribution of sampling ports used for water samples collection, and comparison between experimental and modeled concentrations. Sampling ports are located at sampling levels 2, 3 and 4 and are identified by color dots. Colors are associated to the agreement between measured and simulated particle concentration, based on the coefficient of determination R^2 calculated (**A**) for all times t (0-48 h) and (**B**) for the injection phase only (B).

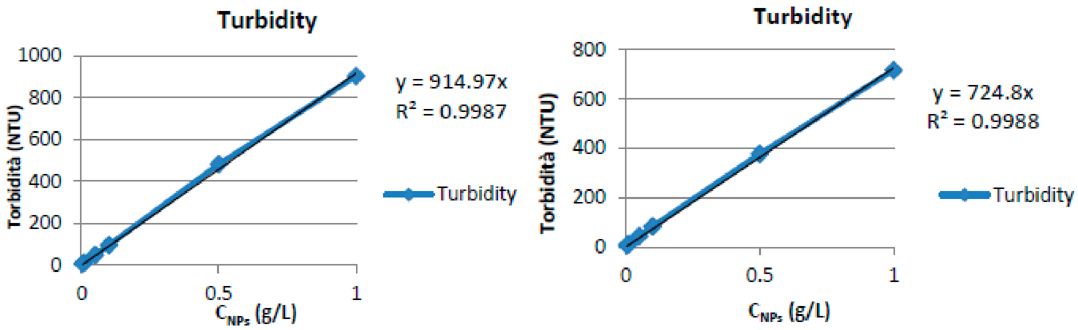

(A) **(B)**

Figure S6. Calibrations to get the NPs concentration from turbidity values. (**A**) the calibration in deionized water, (**B**) the calibration in container inflow.

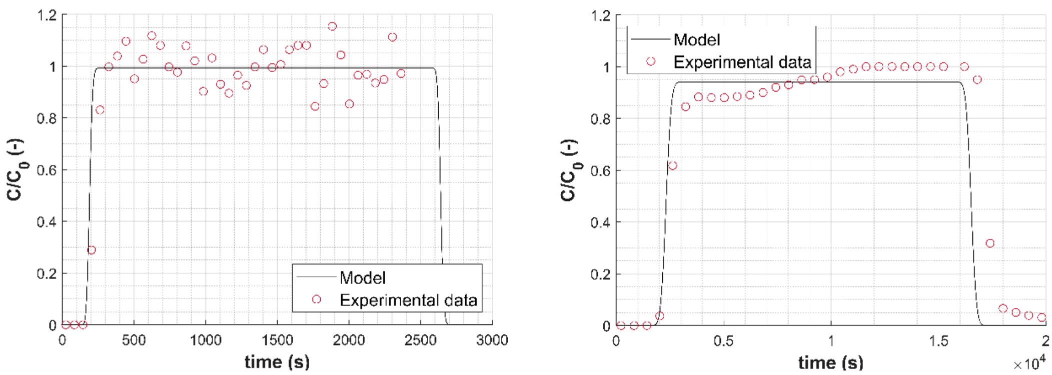

(A) **(B)**

Figure S7. Experimental and modeled breakthrough curves for column transport tests. Tests were performed injecting particles in column having a diameter of 0.025 m and a length of 0.22 m at a concentration of 10 g/L at a Darcy velocity of (**A**) 100 m/d and (**B**) 10 m/d. Tests included a pre-flushing step, a particle injection step, and a post-injection flushing step, all performed at the same flow velocity. The experimental breakthrough curves were modeled using MNMs; linear irreversible attachment was considered (model equations 1-2 in the paper). The partial differential equations for particle transport were solved using a finite differences central-in-space scheme with 200 cells; time derivatives were solved using an Euler implicit scheme with a time step of 2 s. A first type boundary condition was applied at column inlet (C_0 = 10 g/L) and a second type Bc was applied at the domain outlet (zero gradient condition).

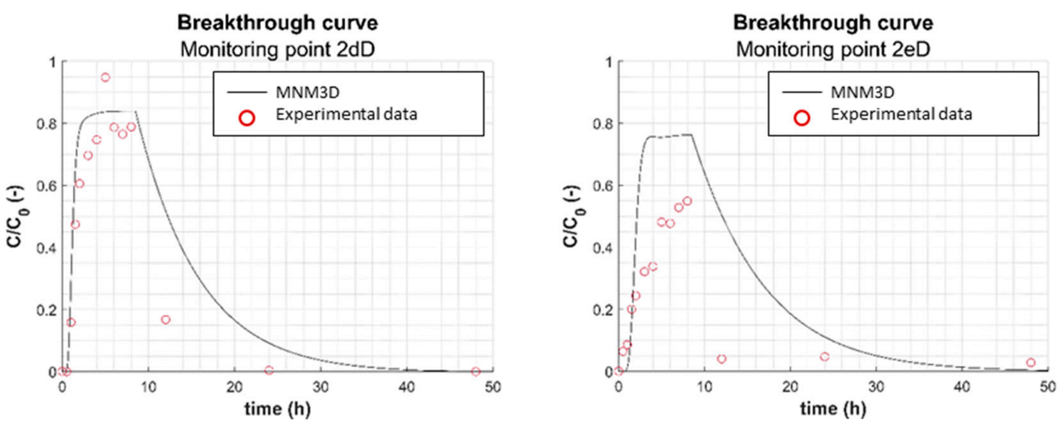

(A) **(B)**

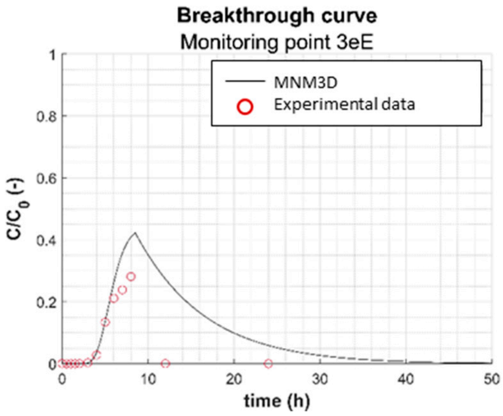

(C)

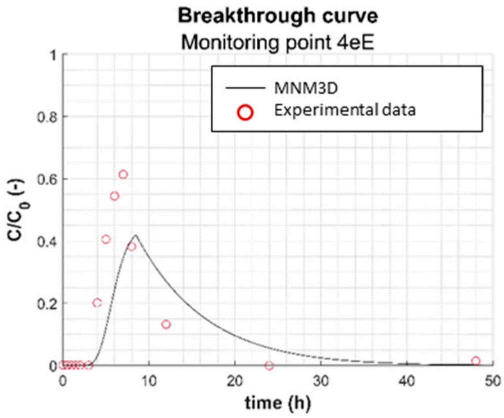

(D)

Figure S8. Breakthrough curves of HA-GoeNPs at the monitoring points (**A**) 2dD (x_{2dD} = 3.5 m, y_{2dD} = 2.98 m, z_{2dD} = 3.31 m), (**B**) 2eD (x_{2eD} = 4.5 m, y_{2eD} = 2.9 m, z_{2eD} = 3.31 m), (**C**) 3eE (x_{3eE} = 4.5 m, y_{3eE} = 2.12 m, z_{3eE} = 2.62 m) and (**D**) 4eE (x_{4eE} = 4.5 m, y_{4eE} = 2.12 m, z_{4eE} = 1.84 m).

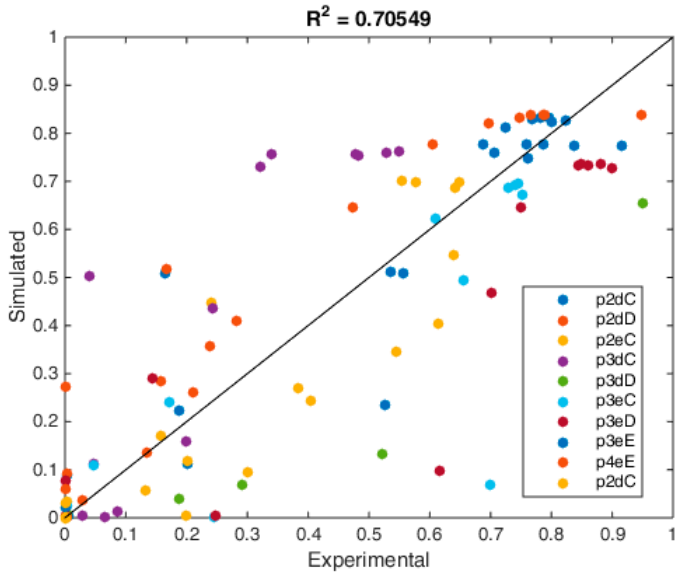

(A)

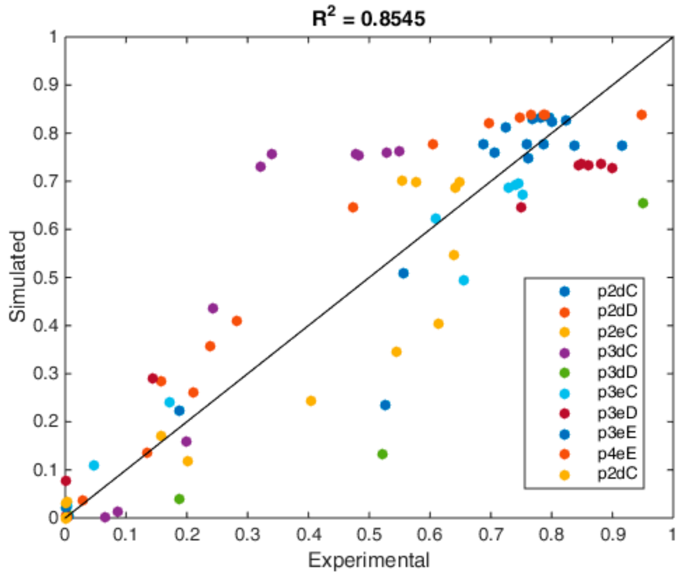

(B)

Figure S9. Correlation graph and global coefficient of determination R^2 calculated for modeled and measured particle concentration at all sampling ports where particles were detected (each identified by a different color). The graph and R^2 are calculated (**A**) for all points and times together (0–48 h) and (**B**) for the injection phase only.